

Pablo FRAILE-JURADO<sup>1,\*</sup>, Juan Carlo MEJÍAS-GARCÍA<sup>2</sup>,  
Maria Esperanza ROLDÁN-MUÑOZ<sup>1</sup>, César BORJA-BARRERA<sup>1</sup>

# Reconstructing the emerged areas of the Mediterranean during the Last Glacial Period: Incorporating bathymetric data and sea level fluctuations

**Abstract:** Fraile-Jurado P., Mejías-García J.C., Roldán-Muñoz M.E., Borja-Barrera C., *Reconstructing the emerged areas of the Mediterranean during the Last Glacial Period: incorporating bathymetric data and sea level fluctuations*. (IT ISSN 0391-9838, 2023). During the last glacial phase, a long and cold period lasting about 100,000 years, the sea level changed in response to climatic variations. However, the position of the sea level cannot be uniquely identified and may vary depending on the duration and intensity of the cold stages within the isotopic subperiods. In this study, we applied a method that integrates a sea-level curve covering the entire glacial period with an elevation model of the entire Mediterranean Sea. The results demonstrate that the shape of the Mediterranean coastlines varied widely over time, with some areas experiencing minor changes while others, such as the Adriatic Sea, the Aegean Sea, and the Strait of Sicily, underwent substantial modifications that resulted in the emergence of large territories for extended periods.

**Key words:** Sea level changes, LGP, Mediterranean Sea, Mapping, Coastline.

## INTRODUCTION

The Last Glacial Phase (LGP), which spanned from approximately 110,800 to 11,700 years Before Present (BP), includes both glacial and interglacial phases (Hughes *et al.*, 2013). It encompasses the Würm glaciation, as well as interglacials corresponding to Marine Isotope Stages (MIS) 5, 3, and 1, and the glacial periods MIS 4 and MIS 2. This period represents one of the most prolonged and coldest phases of the Quaternary climate epoch (Clement and Peterson, 2008; Riechers *et al.*, 2022). This period was characterized by significant fluctuations in Earth's temperature, which resulted in multiple changes in global sea level (Khan *et al.*, 2019). Three distinct isotope stages have been identified within this period (Head, 2021), each exhibiting its own characteristic fluctuations in temperature and sea level (Pérez-Mejías *et al.*, 2019). These fluctuations in temperature and sea level were not constant over time, but instead moved in a complex, dynamic manner. As a result, it is evident that the relative sea level changes that took place

during the LGP cannot be reduced to a single position, but instead must be approached in a comprehensive and detailed manner (Dutton *et al.*, 2022).

Despite the well-established complexity of the LGP, past sea level reconstructions and mapping efforts have often overlooked or not fully captured the intricate variations of this period. The extent of emerged areas during this period has been the focus of extensive research, with maps often depicting the maximum extent of land exposure during the LGM (LGM), which spanned from approximately 26,000 to 19,000 years BP (Hughes *et al.*, 2013; Lambeck *et al.*, 2014), reaching its peak around 21,000 to 18,000 BP (Cooper *et al.*, 2018; Khan *et al.*, 2019; Ishiwa *et al.*, 2019). However, these maps ignore the dynamic and fluctuating nature of sea level changes during the LGP. The extent of emerged areas can vary greatly depending on the shape and depth of the continental shelf, and even a small change in sea level can result in a significant variation in the estimated emerged area (Mann *et al.*, 2019; Björck, *et al.* 2021). This variability underscores the importance of considering the full extent of sea level changes over time, rather than simply reducing them to a single snapshot at 19,000 BP.

The development of an accurate model of the emerged territory during the LGP holds tremendous potential for advancing several disciplines, including paleontology and paleobotany (Ubilla and Martínez, 2016). However, its im-

<sup>1</sup> Departamento de Geografía Física y A.G.R, Universidad de Sevilla, 41004 Seville, Spain.

<sup>2</sup> Departamento de Prehistoria y Arqueología, Universidad de Sevilla, 41004 Seville, Spain.

\* Corresponding author: Pablo Fraile-Jurado (pfraile@us.es)

portance is particularly pronounced in the field of archaeology. In this discipline, one of the goals is to reconstruct the settlements, routes, and distribution areas of past human populations (Mandryk *et al.*, 2001; Sineo *et al.*, 2015; Erlandson and Braje, 2015; Bird *et al.*, 2018). Coastal areas are of particular significance as they often served as important sources of resources for these populations. A detailed and comprehensive model of the emerged territory during the LGM would therefore provide valuable information about the coastal and terrestrial environments available to human populations during this time (Garcea, 2012). This information would play a key role in our understanding of how human populations adapted to and interacted with their changing environments during the LGM.

The objective of this study is to produce a detailed and accurate map of the emerged time of the Mediterranean Sea continental shelf during the LGM. This involves utilizing a bathymetry Digital Elevation Model (DEM) and a curve of past sea levels from 115,000 BP to 6,000 BP. Our approach is since it considers the entire curve of sea levels, rather than simply mapping the maximum extent of emerged lands during the LGM by 19,000 BP as is commonly done by other researchers (Clark *et al.* 2009; Clague and Ward, 2011; Park *et al.*, 2000; Clark and Mix, 2002; Pico *et al.*, 2020). This methodology provides a more comprehensive and nuanced understanding of the emerged territory during the LGM.

## METHODOLOGY AND DATA

In order to calculate the emerged time of each point on the Mediterranean Sea continental shelf during the period from 120,000 to 6000 years BP, a unique methodology was applied. This methodology (Fraile-Jurado and Mejías-García, 2022) involves the application of a custom algorithm to each cell of a bathymetry Digital Elevation Model (DEM) in order to determine the emerged time of each cell during each sub-period of the LGM. The analysis was based on a gridded Digital Terrain Model (DTM) with a resolution of  $1/16 \times 1/16$  arc minutes (approximately 115 m), using mean water depth relative to the Lowest Astronomical Tide (LAT) from EMODnet, complemented by land DTM data in traditional atlas style colours. Although there is no specific information on the vertical accuracy of this DEM, literature suggests that a broad spatial resolution should not significantly impair vertical accuracy. This is particularly relevant in sea level simulations, where vertical precision is less critical in areas with gentle topography, such as coastal or submerged plains (Fraile-Jurado and Ojeda-Zújar, 2013; Li *et al.*, 2023; Talchabhadel *et al.*, 2021).

The equation used to calculate the emerged time of each cell is as follows:

$$tc = (bf - bc) / (bf - bi) \times p$$

Where  $tc$  is the emerged time of a cell for a given temporal period,  $bc$  is the bathymetric elevation of the cell,  $bi$  is the bathymetric elevation of sea level at the start of the period,  $bf$  is the bathymetric elevation of sea level at the end of the period, and  $p$  is the duration of the period in years.

Different subperiods of sea level changes were identified on Barjadí *et al.* (2015) and Silva *et al.* (2017) curve shown in table 1 and fig. 1, corresponding to a simplification of most published sea level curves (Yokoyama *et al.*, 2000; Lambeck, 2001; Yokoyama *et al.*, 2015; Ehlers *et al.*, 2018; Blonder *et al.*, 2018). In order to simplify the sea level curve during the LGM, the periods of rise and fall described in table 1 were identified, resulting in a total of 12 episodes of sea level rise or fall during the 120,000-6000 BP period.

The algorithm was applied to each of the sub-periods of the LGM, and the result of this application was a raster layer in which the emerged time in years of each cell is represented. The minimum value (0) in the layer indicates that the cells were always submerged during the period, while the maximum value represents cells that were emerged throughout the entire period, corresponding to the duration of the period in years.

In regions where Benjamin *et al.* (2017) discerned either subsidence or uplifting trends spanning the past 120,000 years, a continuous rate of vertical movement was assumed, as described by the equation:

Here,  $Lt$  represents the local trend,  $VM$  denotes the vertical movement in mm, and the denominator of 120,000 years signifies the duration of the analyzed period. The rates calculated from this formula were subsequently adjusted in areas exhibiting tectonic activity, sedimentation, or erosion, as identified by Benjamin *et al.* (2017). Notably, the maximum rate of change observed was a mere 0.075 mm/year, indicating minimal vertical movement over the specified timeframe. To visually represent these uplift and subsidence trends, a raster surface was generated from the data provided by Benjamin *et al.* (2017), where the annual rate of sea level change due to uplifting or subsidence is mapped (fig. 2). A spatial interpolation technique based on IDW (Setianto and Triandini, 2013) was employed to smooth the values, ensuring that the localized measurements were distributed in a coherent manner across the study area. This technique provides a gradual transition between points of measurement, avoiding abrupt changes in the interpolated surface. The resulting raster layer was then integrated into the model by summing the annual rates of vertical movement with the sea level values at each grid cell for any given subperiod from table 1. However, given the extremely low rate of vertical movement observed – less than +0.075 mm/year – its influence on the overall sea level curve is negligible when compared to the much larger changes observed in global sea level trends during the LGM.

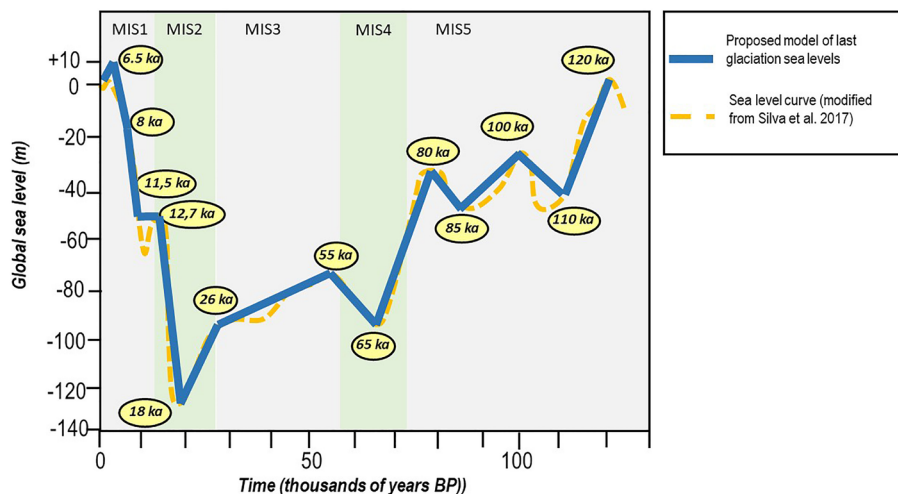


Figure 1 - Applied sea level curve and marine isotope stages.

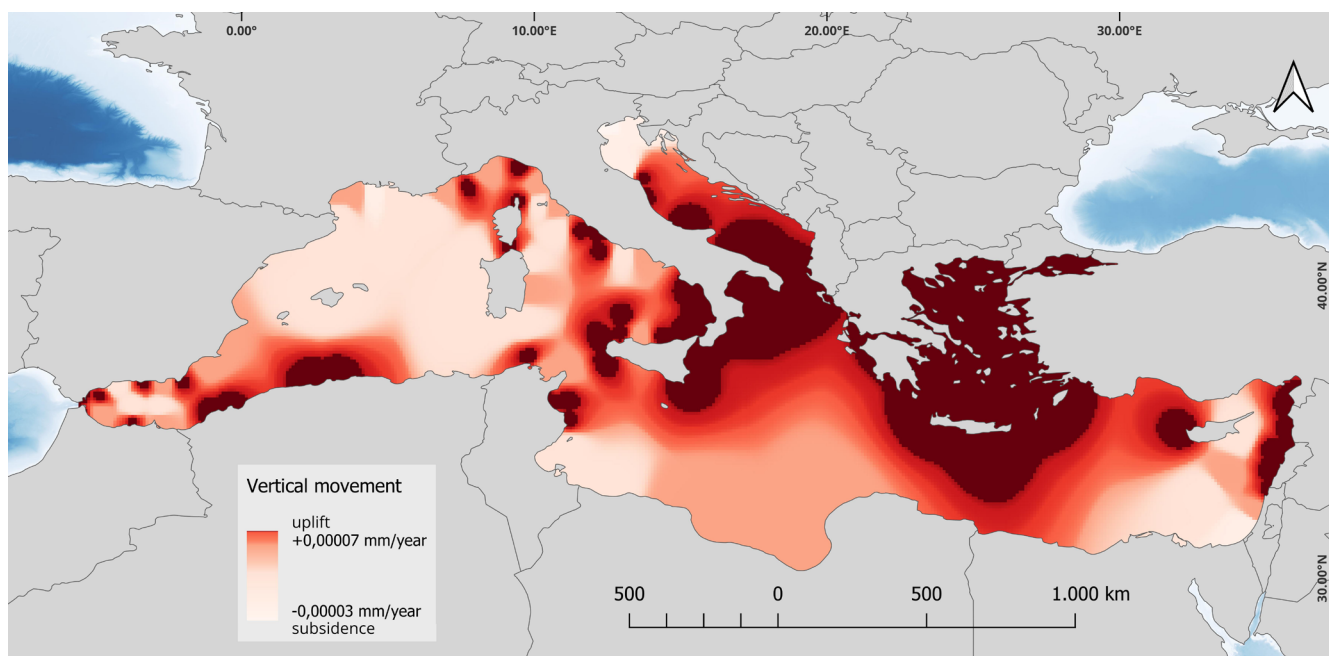


Figure 2 - Interpolated surface of vertical movements based on Benjamin *et al.* (2017).

Table 1 - Identification of sub-periods from the sea level curve of Barjadí *et al.*, (2015) and Silva *et al.* (2017).

Subp.	Period	Series/Epoch	MIS	Begin (ka.)	End (ka.)	Ratio (m)	Final depth (m)	Annual trend (mm/year)
1			5d	120	110	-45	-45	-4.50
2	Lower Paleolithic		5c	110	100	+20	-25	+2.00
3			5b	100	85	-25	-45	-1.30
4	Middle Paleolithic	Upper Pleistocene	5a	85	80	+15	-30	-3.00
5			4	80	65	-65	-95	-4.30
6			3	65	55	+20	-75	-2.00
7	Upper Paleolithic			55	26	-15	-90	-0.52
8			2	26	18	-40	-130	-5.00
9	Epipaleolithic/ Mesolithic			18	12.7	+75	-55	+14.20
10					12.7	11.5	0	-55
11	Neolithic	Holocene	1	11.5	8	+30	-25	+8.60
12					8	6	+25	0

Source: adapted from Zazo (2015) and Silva *et al.* (2017).

While these changes are not significant in the final results for the temporal and spatial scales chosen in this study, the vertical correction based on Benjamin's results was included as a standard procedure to ensure the replicability and precision of results, especially in smaller-scale studies or regions where vertical crustal movements may have greater local significance.

Finally, in order to determine the total surface area of emerged time for the sea floor of the Mediterranean Sea during the LGP, the generated raster layers were summed. This resulted in a detailed and accurate map of the emerged time of the Mediterranean Sea continental shelf during the period from 120,000 to 6000 years BP. Although the onset of the Holocene 11,700 years ago is commonly used to mark the end of the LGP, the study period extends to 6000 BP because until then sea level continued to rise to a position similar to present-day (Mörner, 2021).

## STUDY AREA

The Mediterranean Sea covers a surface area of 2.51 million km<sup>2</sup> and measures almost 4000 km in length, making it the second largest enclosed sea in the world. Despite its large size, the Mediterranean has a relatively deep average depth of about 1,300 m, with a limited development of the continental shelf. However, the continental shelf exhibits a great diversity of shapes and development patterns (fig. 3).

Due to the particularities of this work, in which the study area is delimited to the maximum extension of the emerged surface when the sea level reached its lowest position (between -120 and -130 m), the continental shelf will be considered as the area between the -130 m isobath and

the current coastline, although geologically the extension and depth of the continental shelf may be much larger. Observing the frequency histogram of the continental shelf (fig. 4), it can be seen that the depth distribution is relatively homogeneous, with a lower predominance of shallow and very deep areas, less than -100 m.

In order to analyze the broad Mediterranean continental shelf in greater detail, three study sectors (Western, Central, and Eastern) were identified, corresponding to areas 1, 2 and 3 in fig. 4. Besides producing maps with greater visual detail, frequency histograms of the number of years emerged were also generated. Additionally, due to the singularity of certain spaces owing to their insularity or the fact that they are coastal areas with different bathymetries from the Mediterranean average, specific analyses were carried out in the Balearic Islands (4), Corsica and Sardinia (5), the Strait of Sicily (6), the Adriatic Sea (7), the Aegean Sea and the coasts of Greece and Turkey (8), and the Gulf of Iskenderun and Cyprus (9).

The Spanish side of the Mediterranean Sea is characterized by a varied topography of its continental shelf. On the extreme western Mediterranean, both the northern and southern coasts of Andalusia and Morocco display a narrow continental shelf, as reported by Lafosse *et al.* (2018) and Lobo *et al.* (2006). The island of Alborán, situated between both coasts, is relatively small, measuring only 660 m in length, but has an exceptionally extended continental shelf of approximately 60 km. Along the southern coast, the continental shelf widens slightly between the cities of Melilla (Spain) and Oran (Algeria). However, on the northern coast of Spain, the shelf remains narrow until the areas between the Capes of Palos and Cape of la Nao, where it expands to approximately 40 km wide. This increase in



Figure 3 - Study area.

Figure 4 - Bathymetry of the Mediterranean Sea.

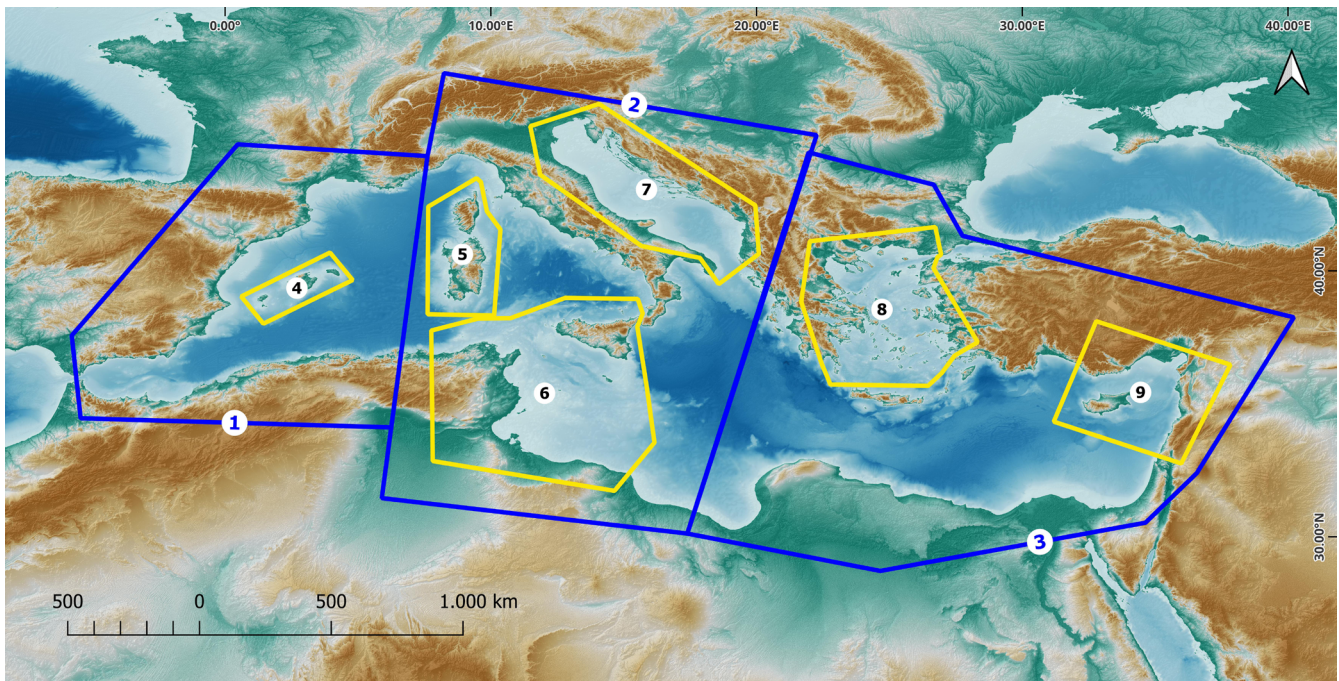
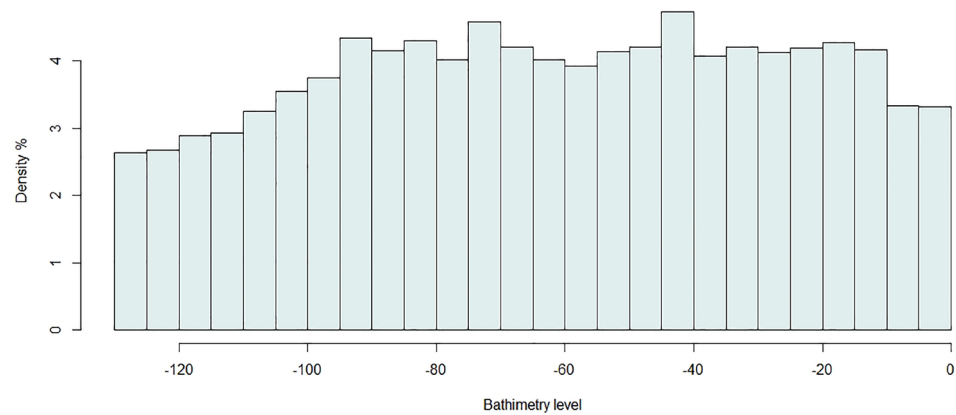


Figure 5 - Specific analysis areas.

width continues until the delta of Ebro in Cataluña, where one of the widest continental shelves of the Mediterranean Sea can be found.

In addition to the previously mentioned characteristics, the Balearic Islands in the Spanish Mediterranean Sea (area 4 in fig. 5) also exhibit a unique feature in their bathymetry and geology. The continental platform surrounding these islands is nearly continuous, connecting the islands of Mallorca and Menorca, as well as Ibiza, Formentera and Cabrera. This distinct feature adds to the varied and complex bathymetry of the Spanish Mediterranean continental shelf, a characteristic that is also observed in the region between Malta and Sicily, highlighting the importance of further study in both areas.

A narrow continental shelf can be found in most of Catalonia (Ercilla *et al.*, 1995), where some mountain ridges are

very near the shoreline, making the shelf narrower. It gets much wider in the Gulf of Lion (Badhani *et al.*, 2020), where thick sediment strata can be found (Rabineau *et al.*, 2005).

The Gulf of Genova coastline is characterized by a narrow continental shelf, as noted by Enrichetti *et al.* (2020). The continental shelf slightly widens only between Livorno and Naples, in the western part of Italy, as reported by Antonioli *et al.* (2017). The latter authors also highlighted the influence of extensional tectonics in response to the eastward roll-back of the west-directed Apennine subduction in the areas. Corsica (area 5 in fig. 5) has a very narrow continental shelf that merges to the south with Sardinia. On the other hand, in Sardinia, a strong structural control on the shape of the continental shelf has been identified, with the presence of volcanic rocks and fossil paleo-valleys, according to Deiana *et al.* (2021).

The continental shelf of the Adriatic Sea (area 7 in fig. 5) has been the subject of numerous studies for several decades due to its shallow depth, often less than 40 m, and the richness of benthic communities (Colantoni *et al.*, 1979; Malanotte-Rizzoli, 1991; Donnici and Barbero, 2002, Marchese *et al.* 2020, Pellegrini *et al.*, 2021, Vilibic *et al.* 2020, Lipej *et al.* 2022) This is the result of the interaction between deltaic areas and marine sediments. The Adriatic Sea is a semi-enclosed basin located in the central Mediterranean, which has undergone significant geological changes over time.

The eastern coasts of Tunisia feature a wide continental shelf that connects the Gulf of Gabes and the Gulf of Hammamet with the islands of Djerba, Sharqi, Lampedusa, and Malta with Sicily (area 6 in fig. 5). The shoreline morphology is dominated by sandy beaches and rocky headlands, with several hard rock outcrops. The northern coast of Tunisia is characterized by a poorly defined boundary between the Nubia and Eurasian plates (Halouani *et al.*, 2012). The offshore continental margin is believed to be part of the North Africa collisional fold and thrust belt system, linking the Maghrebian and Sicilian-Apennine chains. The deformation zone on the Tunisia margin is influenced by gradual NW-SE convergence, with limited and sporadic seismic activity, unlike the regions of northern Algeria and northern Sicily (Camafort *et al.*, 2022). The continental shelf of Algeria and Morocco is mostly underdeveloped due to the presence of mountain ranges that form a structurally-controlled edge and subduction contact between the Eurasian and African plates (Domzig *et al.*, 2006). This region is contiguous with the area between Oran and Melilla.

The Greek continental shelf is strongly structurally controlled due to the proximity of mountain ranges, showing a narrow profile and generally similar to the current coastline on its western side. The Aegean Sea continental shelf (area 8 in fig. 5) is much more complex and has been the subject of numerous studies, partly due to the territorial disputes between Greece and Turkey in delimiting maritime spaces (Gros, 1977; Georopoulos, 1988; Acer, 2017). It is a sea of great tectonic complexity, with numerous faults delimiting different basins of greater depth (Foutrakis and Anastasakis, 2020).

The southern coast of Turkey (area 9 in fig. 5) features a narrow continental shelf that closely resembles the current coastline due to the presence of nearby mountain ranges. However, a much wider continental shelf can be observed only in the area between Mersin and the Gulf of Iskenderun, where the latter is filled with thick sedimentary sequences from prograding deltas (Ergin *et al.*, 1996).

The coastlines of Cyprus, Lebanon, Syria, and Israel are characterized by a very narrow continental shelf that only widens in Egypt. Thick sedimentary facies of metric and submetric thickness have been found in Egypt at considerable distances from the current Nile River delta, indicating powerful accretion and erosion processes in the region

(Kholeif and Ibrahim, 2010). Erosion has been the dominant process in the area over the last century, as identified by Frihy *et al.* (1991).

The coastal areas of Egypt and Lebanon exhibit a narrow continental shelf that extends to the Gulf of Sidra, and has been the subject of various legal studies regarding territorial waters (Leanza, 1993; McGinley, 1985; Roach and Smith, 1994).

## RESULTS

The results of the study are summarized in fig. 5, which provides a clear visual representation of the findings. Upon initial inspection, it is evident that most of the Mediterranean coasts have had a similar profile to the current configuration due to their generally underdeveloped continental shelves. However, there are some areas that have experienced prolonged periods of emergence, particularly in the eastern coast of Tunisia and the northern region of Egypt, where cell units with values close to or even greater than 100,000 years of emergence are common. Additionally, the Adriatic Sea has a large area where a significant number of cell units have emerged for moderately long periods, ranging from around 20,000 years to values close to 100,000, although the majority of these are located near the current coastline. These findings shed light on the complex geological history of the Mediterranean coasts and the impact of sea-level changes over time. Below are presented the results obtained distinguishing between the different sectors of the Mediterranean Sea: western, central, and eastern.

Fig. 7 displays that in general, three types of emerged time values are observed with a much higher frequency than the rest: those below 10,000 years, corresponding to very low sea level positions reached only during the LGM, intermediate values between 55,000 and 65,000 years, and high emerged time values with cells above 105,000 years.

In the southern Andalusian coast (fig. 8) the emerged surfaces during the studied period were limited to a few areas, with a wider near Cape Gata. The Mar Menor was barely submerged throughout the entire studied period. In the sector from Cape Nao to the Mar Menor, an extensive area of approximately 40 km was emerged for brief periods associated with the Glacial Maximum, ranging between 20,000 and 10,000 years. The Ebro Delta is a unique feature, with shallow depths around it that also exhibit values of more than 90,000 years of emergence. To the south of the delta, a narrow strip of less than 10 km has been emerged for more than 100,000 years, and wider areas emerged for shorter periods. The Columbretes paleo-island was identified, with a maximum area emerged for 60,000 years.

Regarding the rest of the western coasts of Tunisia, Algeria, and Morocco, there are few noteworthy areas due to the high similarity between any past coastline and the present one for most of the glacial period. The island of

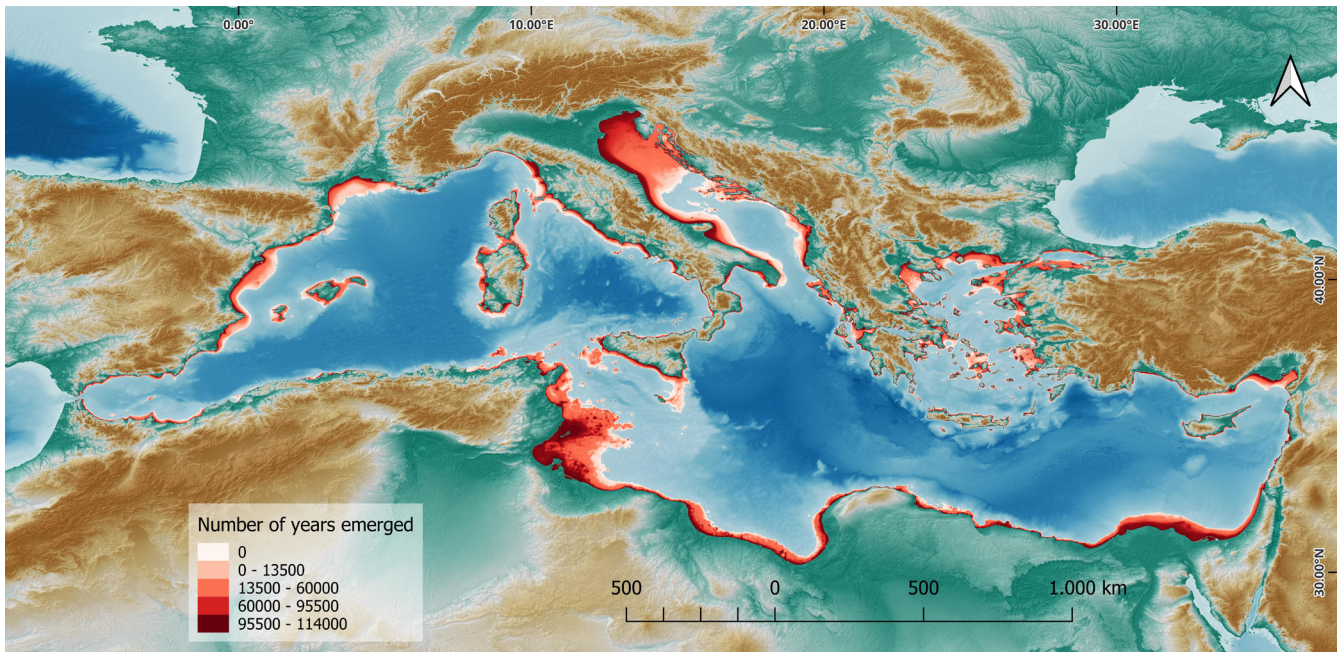


Figure 6 - General map of results for the entire Mediterranean Sea. The results are presented as the number of years emerged.

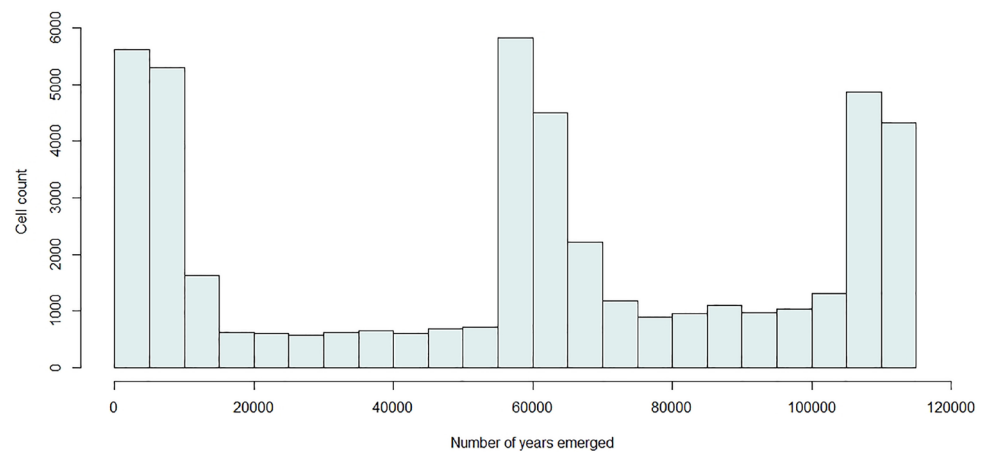


Figure 7 - Frequency histogram for the entire Mediterranean.

Alboran, currently a 600 m islet, reached lengths of nearly 30 km during the study period, although for most of the time it remained around 20 km.

The Gulf of Lion exhibits decreasing values from the current coastline, such that although it is possible to identify ancient shorelines more than 40 km from the current line, the values identified in its surroundings are often less than 20,000 and even 10,000 years, indicating that they were emerged for a very short period during the LGP. To identify much higher values and those close to 100,000 years, it is necessary to observe the cells close to the current coastline.

Fig. 9 displays a similar structure to that of fig. 6 (for the entire Mediterranean), with the difference being that the relative extent of territories that were emerged for more than 105,000 years is much lower, approximately half of that observed for the entire Mediterranean.

The Balearic Islands appear as a pair of two macro-islands, especially Mallorca-Ibiza, in addition to Menorca-Formentera-Cabrera, which were emerged for periods exceeding 60,000 years. During the maximum cold event about 18,000 years ago, the extent of both islands was practically double that of today. In any case, this large extent was above sea level for a relatively short period of time, since similar results to those discussed for fig. 6 are observed in fig. 10 for the Balearic Islands, where the lower frequency of cells with values exceeding 105,000 years is even more pronounced.

The results obtained for the Central Mediterranean (fig. 11) area are similar to those observed in fig. 6, but with a greater emphasis on periods with values exceeding 90,000 years and especially 105,000 years (fig. 12). This is reflected in the map of fig. 11 with the large areas of emerged continental shelf observable for long periods of time in the northern

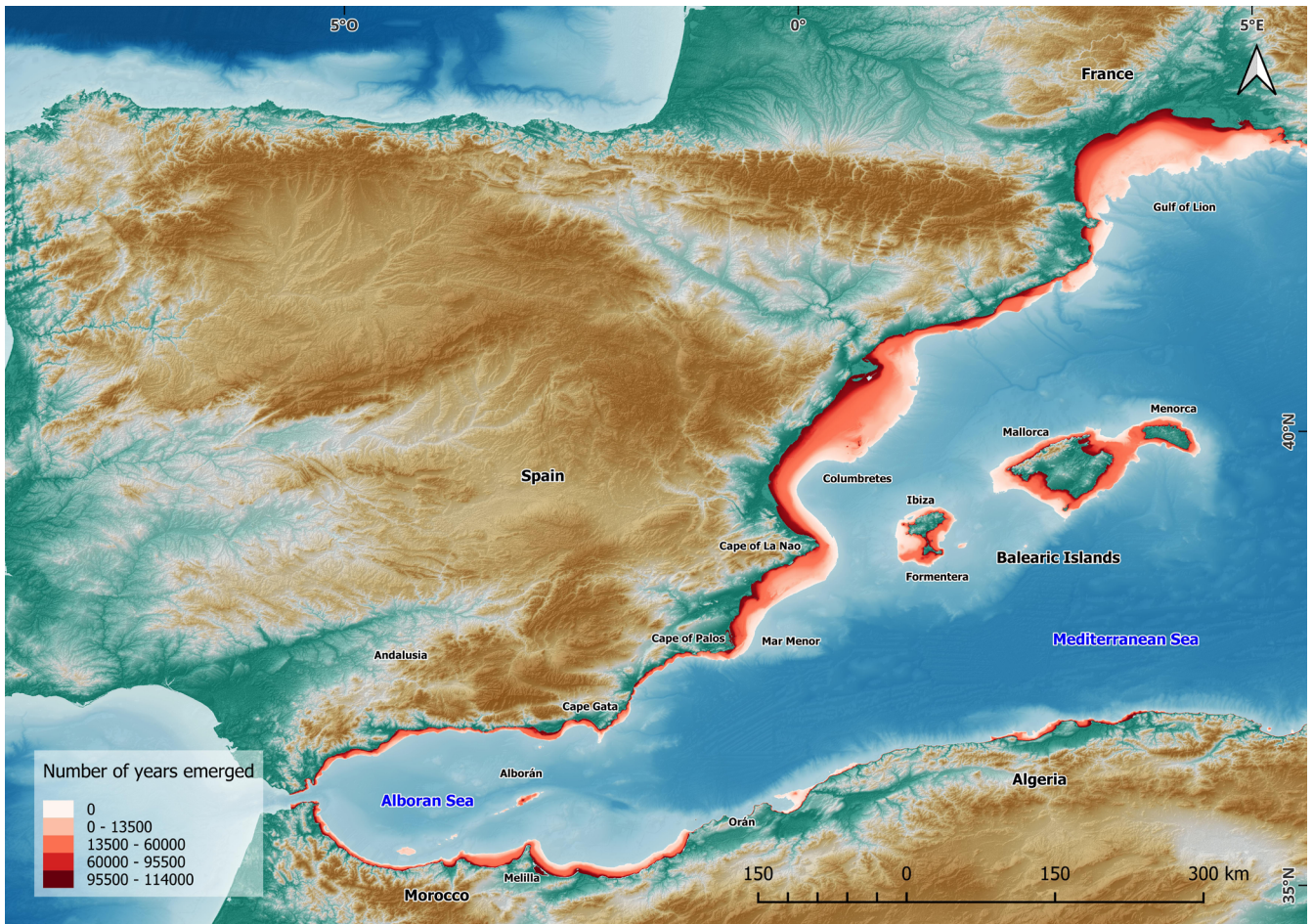


Figure 8 - Results obtained in the western Mediterranean. The results are presented as the number of years emerged.

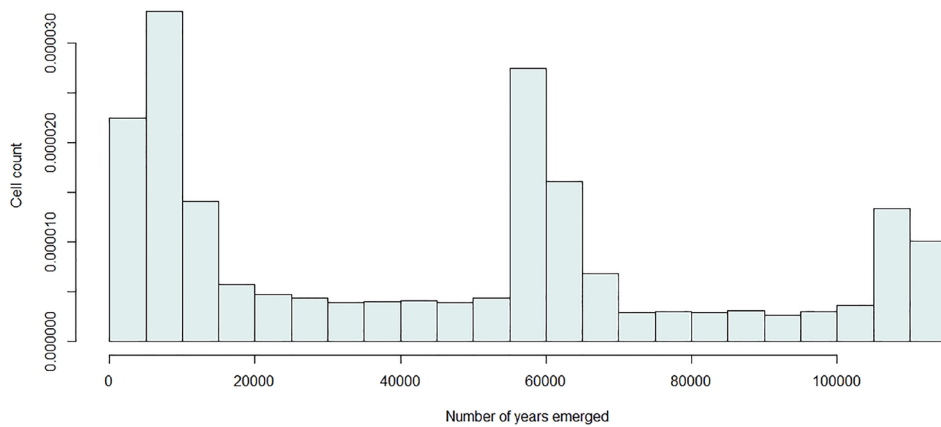


Figure 9 - Frequency histogram obtained in the Western Mediterranean (area 1 in fig. 5).

Adriatic and in the Sicilian Channel, and to a lesser extent between Corsica and Sardinia and in the Gulf of Taranto.

The western coast of the Italian peninsula is characterized by the continuous presence of significant promontories that no longer exist, which have connected, for periods exceeding 40,000 years, the current islands of Elba, Toscana, Montecristo, Ischia, and Capri, forming a uniquely rugged and dotted with prominent capes coastline.

In Corsica and Sardinia (fig. 13), a similar situation to the Balearic Islands is observed, with a large number of cells that were emerged for periods shorter than 15,000 years, another large group of cells emerged during 55,000 to 65,000 years, and a more extensive group than that of the Balearic Islands emerged for more than 100,000 years. Sardinia, in particular, shows the existence of at least two wide promontories that penetrate the sea both to the east and



Figure 10 - Frequency histogram obtained in the Balearic Islands (area 4 in fig. 5).

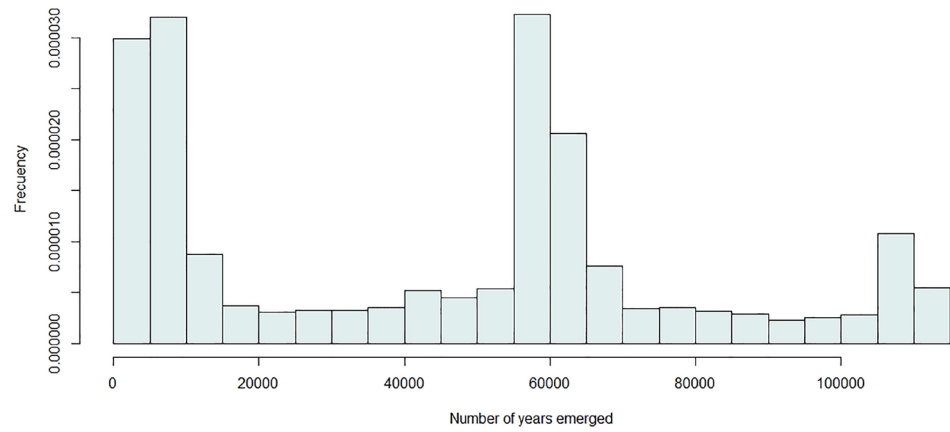


Figure 11 - Results obtained in the central Mediterranean. The results are presented as the number of years emerged.

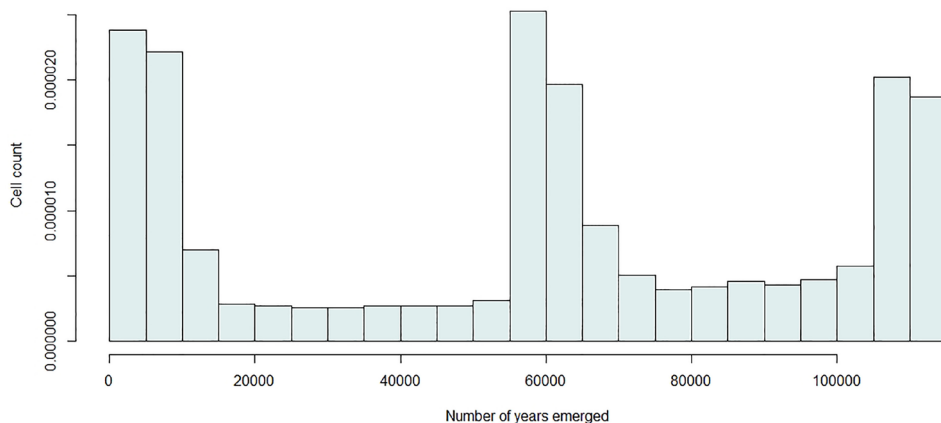


Figure 12 - Frequency histogram obtained in the Central Mediterranean (area 2 in fig. 5).

to the west (fig. 11), which do not exist today and bear no resemblance to the current coastline, as well as the emergence of all its current bays.

The Gulf of Taranto exhibits little variation along the LGP with respect to the current coastline. However, the Adriatic Sea showed a completely different shape throughout the entire study period. In its southern half, the Gulf of Manfredonia was emerged for periods exceeding 80,000 years during which the Gargano Peninsula was virtually nonexistent as a peninsula, since its shape was much rounded (fig. 11). The western shore of the Adriatic east of Italy displays areas up to 20 km wide that have been emerged for periods exceeding 80,000 years, while on the other side, the Croatian coast has significantly less emerged time. Nonetheless, most of the islands that currently make up the Croatian coast remained connected forming a probably longitudinal coast for several tens of thousands of years.

In the case of the Adriatic Sea, it can be observed that not only are the peaks common to other histograms around 60,000 years and above 105,000 years slightly higher (fig. 14), but also all values between 65,000 and 105,000 years, which is consistent with the results observed in the Adriatic in the map shown in fig. 9. The northern half of the Adriatic was emerged for extended periods of time, although only values exceeding 80,000 and even 100,000 years are identified in the vicinity of the current coastline. Based on the obtained results, it is likely that an archipelago with an east-west orientation existed for several tens of thousands of years, which penetrated the Adriatic Sea almost opposite to the direction of the current Croatian coast.

Both the Strait of Messina and the Strait of Sicily remained open throughout the entire glacial period. However, they were considerably narrower than they are today. The Strait of Sicily or Sicilian Channel must have been dotted with large islands that no longer exist, located both to the southwest and southeast of the island. The latter was connected to Sicily as a peninsula for at least 15,000 years (fig. 15). On the coasts of Tunisia, apparent plains that must have existed for most of the study period stand out, connecting the current continental surface with the island of

Kerkennah, forming a large peninsula that was above sea level for more than 80,000 years, and commonly for more than 100,000 years (fig. 16). A similar situation occurred further south with the island of Djerba.

Despite the presence of a large number of islands, the results obtained in both Greece and western Turkey (fig. 16) show little difference between the current coastline and the emergent areas during the LGP. However, it is worth noting that values ranging from 20,000 to 40,000 years of emersion are frequently found in the northernmost part of the Aegean Sea, while some islands such as Lesbos, Samos, and Ikaria remained connected to the Anatolian Peninsula for almost the entire glacial period. In the Aegean Sea, a large central island appeared that for at least 20,000 years aggregated the islands of Naxos, Paros, and Ios, with the first two being connected during most of the glacial period. It should be noted that both the Dardanelles Strait and the Bosphorus Strait remained closed for periods exceeding 80,000 years, disconnecting the Mediterranean Sea from the Black Sea. In the Eastern Mediterranean, the values below 10,000 years are the lowest among all the analyzed territories (fig. 17). The maps obtained reveal some other relevant changes in the shape of this sector of the Mediterranean coastlines over time. The closure of the Gulf of Corinth, the connection of the island of Euboea to the mainland, along with the significant closure of its northern and southern gulfs, and the unification of the Ionian islands of Kefalonia and Zakynthos are some of the notable examples.

Fig. 16 shows that the Gulf of Iskenderun remained emerged during most of the LGP. However, the rest of the eastern Mediterranean coastlines had a similar form to the present day. The island of Cyprus always remained disconnected from the Asian continent and barely shows any significantly different features from the current ones that were emerged at any point during the study period. However, large areas remained emerged off the current coasts of Israel and Egypt, particularly the Sinai Peninsula. Most of these areas were emerged for periods of time exceeding 55,000 years, with very few cells showing values much lower than 10,000 (fig. 18).

Figure 13 - Frequency histogram obtained in Corsica and Sardinia (area 5 in fig. 5).

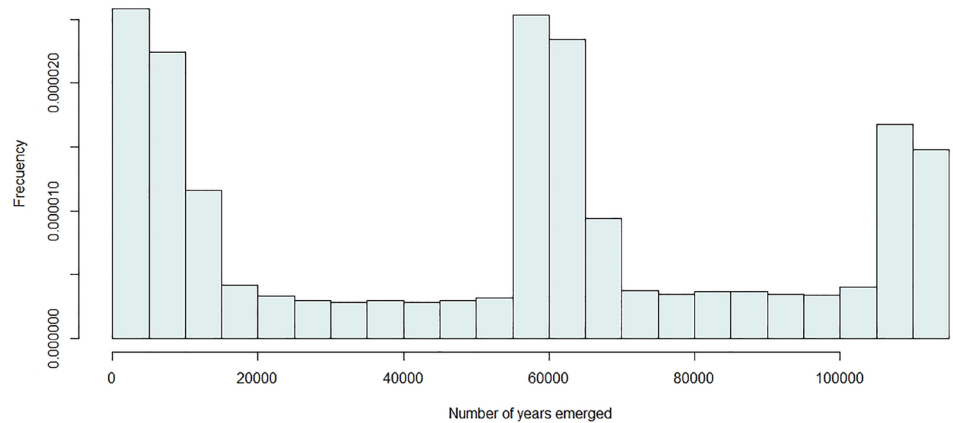


Figure 14 - Frequency histogram obtained in the Adriatic Sea (area 7 in fig. 5).

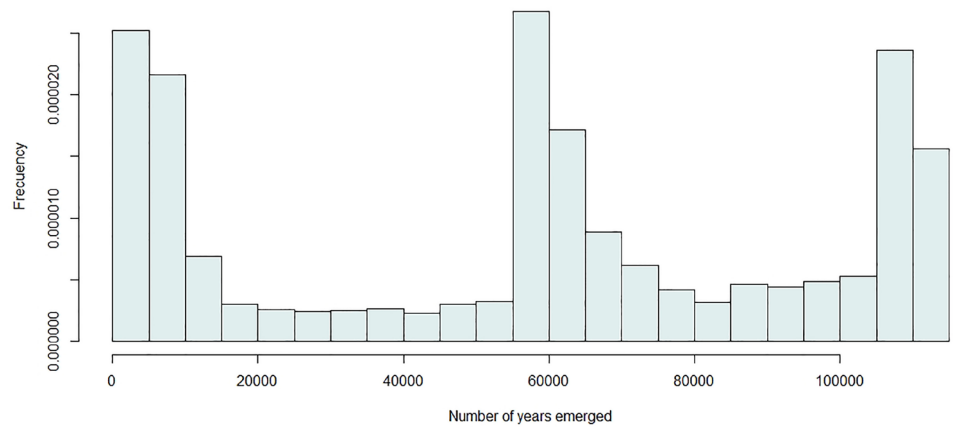
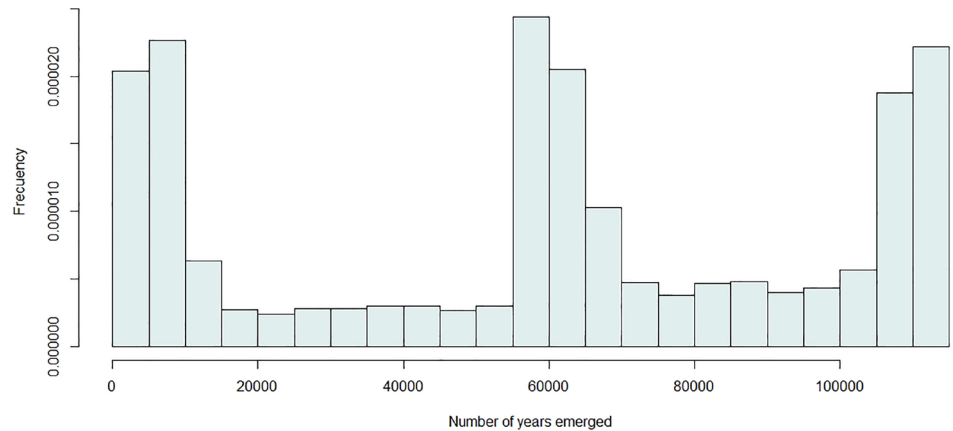


Figure 15 - Frequency histogram obtained in eastern Tunisia and Sicily (area 6 in fig. 5).



## DISCUSSION

The applied method has proven to be highly effective in identifying the emerged areas with greater precision than traditional approaches. In fact, a comparison with other methods – such as identifying a single coastline during the maximum glacial period 18,000 years ago or assuming a linear descent and ascent throughout the entire study period – was conducted in a previous study, demonstrating the superior accuracy of this approach (Fraile-Jurado and Mejías-García, 2022).

The authors are aware of the weaknesses of the method, which focus on two elements. The first is assuming that the

current digital elevation model of the bathymetry is the same as that during the entire LGP. In certain study areas where, for example, sedimentary inputs may have been significant (such as the Nile Delta), the results obtained must be interpreted with extreme caution. The second element is that the sea level curve used, composed of 12 sub-periods, is not necessarily the most accurate possible. However, regarding the method, the advantage is that it admits improvements in both areas: the incorporation of a bathymetric DEM from any past date, which has been nonexistent at least for the scale of the study presented, as well as improvements in the accuracy of the sea-level change line, which would allow for a



Figure 16 - Results obtained in the eastern Mediterranean. The results are presented as the number of years emerged.

more precise algorithm. In the opinion of the authors, at the scale of the study performed, neither the vertical precision nor the spatial resolution of the DEM appear to be relevant. Modeling changes in bathymetry and generating different DEMs have only been successful in areas much smaller than the one addressed in this paper. This approach is particularly effective when sedimentation processes outweigh erosion, as demonstrated in the study of Lodolo *et al.* (2022) on the Adventure Plateau. While other authors (Yao *et al.*, 2009) have attempted to model erosion and deposition processes using less accurate techniques, their applicability to areas as large as the one of this paper is highly questionable.

Another potential limitation of the study conducted is the exclusive use of a bathymetric DEM, without accounting for factors such as local tectonics or compensation due

to post-glacial rebound, except for the inclusion of vertical compensation data where available. While there are local studies on tectonics and vertical movements within the Mediterranean domain, the distribution of high quality data is non-uniform across the region. The data from Benjamin *et al.* (2017) are limited in spatial resolution and show a very limited impact in the analysis. Consequently, akin to the treatment of deltaic areas, this leads to non-continuous modifications of the DEM, resulting in outcomes not derived from a singular methodology. Furthermore, although models of post-glacial rebound cover the entire Mediterranean study area, their application was disregarded for two reasons: a) there exist uncertainties regarding the characteristics and even the direction of post-glacial rebound in this region (Segev *et al.*, 2006), and b) over periods spanning a few thou-

Figure 17 - Frequency histogram obtained in the eastern Mediterranean (area 3 in fig. 5).

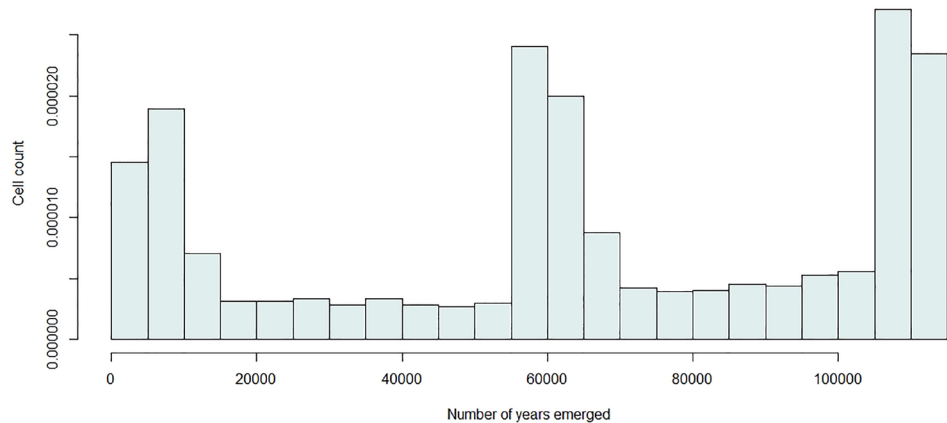
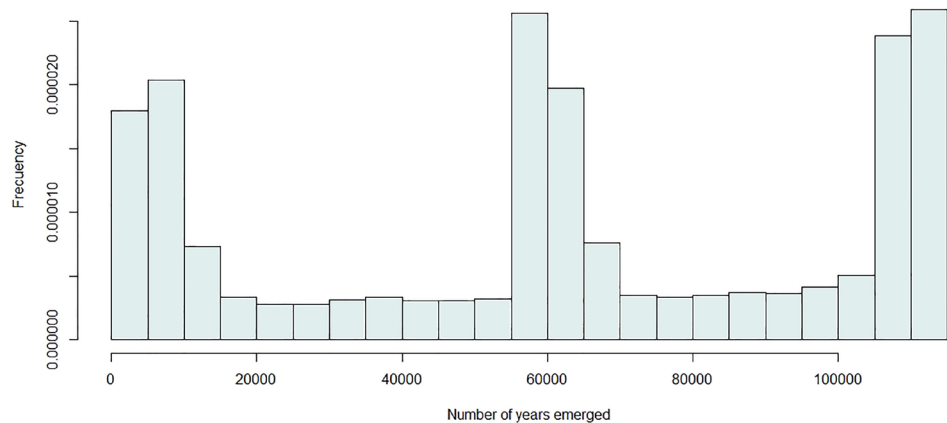


Figure 18 - Frequency histogram obtained in Cyprus and the Gulf of Iskenderun.



sand years (since the LGM), the accumulated changes from post-glacial rebound and other local factors such as tectonics are minor compared to the magnitude of sea-level changes addressed in the article (Ostanciaux *et al.*, 2012, Benjamin *et al.*, 2017). This rationale underpins the decision to focus solely on sea-level changes during the last glaciation and a bathymetric digital elevation model, thus arguing against the inclusion of global considerations like the ICE3G (Peltier, 2002), ICE5G (Argus and Peltier, 2010, Simon *et al.*, 2015), or ICE6G models (Ding *et al.*, 2019).

Although the histogram of frequencies of the continental shelf shows a relatively homogeneous distribution of depths, with a lower prevalence of shallow and very deep areas, there are areas that emerged during different times, mostly due to the size and depth of the continental shelf and its relationship with changes in sea level. The curve used in this article describes these changes, but relating current bathymetry to past sea level curves is not a task than can be seen by a visual inspection due to the complex curve over geologic time and the poorly known three-dimensional surface of the shore platform. A tool that can merge both sources of information into a single map is useful for geographical knowledge and other disciplines, but this topic is not widely discussed in the specialized scientific literature, making it difficult to have an appropriate discussion about this work.

Regarding the interpretation of the forms of all the histograms obtained, which show three peaks around values

of less than 10,000 years, around 60,000 years, and above 105,000 years, it seems to depend much more on the characteristics of the sea level curve used than on the characteristics of the bathymetry. Comparing any of these histograms with the depth frequency histogram in fig. 5, it is evident that the bathymetry, from the point of view of the entire Mediterranean, is relatively smooth and homogeneously distributed throughout the sea. However, local results show that detailed studies are necessary to make a less general interpretation.

This study differs from other scientific articles that have used isobaths of -120 or -130 m to identify all the emerged areas during the LGP (Clague and Ward, 2011; Clark and Mix, 2022; Pico *et al.*, 2020). However, there are few authors who have examined changes in sea level positions over extensive periods with greater precision. For example, Lambeck's works (1995 and 1996) are characterized by their extreme rigor, which represents all the sea level positions in different maps in different regions. This study's main contribution lies in synthesizing all sea level positions into a single map, reducing the need for multiple maps proposed by Lambeck.

The Gulf of Lion and the Adriatic Sea are excellent examples of continental shelves where the value of -120 is far from the current coastline. However, due to the shape and structure of the continental shelf, during most of the LGP, these areas were situated in an intermediate position between the current coastline and the -120 m isobath, highlighting the importance of the spatial analysis conducted in this work.

The importance of deltaic areas must be accurately measured. It is unquestionable that in large deltaic areas such as the Nile and to a lesser extent, the Ebro, Po, or Rhône estuaries, changes must necessarily be significant. However, there is currently no public digital elevation model of these territories that adequately models the transformations undergone over time. Therefore, and even emphasizing the risks of using the bathymetric DEM for these territories, it is currently the only option to consider, despite the errors that may be significant. While the Mediterranean basin is known for having fewer large river basins compared to other regions in the world, it may be advantageous for the application of the methodology presented in this study. Apart from the Nile basin, which spans over 3 million km<sup>2</sup>, only a few basins such as the Rhône, Ebro, Po, and Muluya exceed 70,000 km<sup>2</sup> in size. Therefore, the Mediterranean basin seems to be a suitable location for the development of this methodology, since its basin has relatively few deltaic areas compared to other regions, which suggests that modifications to the bathymetry may be smaller and easier to identify.

The study highlights the dramatic changes that many important narrow straits of the Mediterranean Sea have undergone. While some narrow straits of particular historical and hydrodynamic relevance, such as Gibraltar, Messina, or Sicily, never closed, this work identifies that according to the methodology and data employed, narrow straits like the Dardanelles and numerous connections between mainland and islands remained closed for variable periods ranging from 20,000 to 80,000 years. Although many authors have addressed this issue both in the Mediterranean (Çağatay *et al.*, 2000, Thiede, 1978, Vergnaudgrazzini *et al.*, 1989) and in other territories (Coronato *et al.*, 2004, McCulloch *et al.*, 2005), most studies approach it from the perspective of a single minimum of around -120 m 18,000 years ago, ignoring the enormous spatiotemporal variability highlighted in this work.

## CONCLUSIONS

During the last glaciation, the Mediterranean Sea was a continuous water mass only disconnected from the Black Sea. However, some of its present-day coasts were dramatically different from those that existed during the last glaciation. The study reveals not only equidistant extensions of the current coastline, but also a great amalgamation of peninsulas, capes, bays, and isthmuses that were emerged or submerged during different periods of time. This extreme variability in the shape of coastlines underlines the importance of conducting studies that consider all fluctuations of sea levels on the continental shelf.

Although the method used has obvious limitations by not considering possible changes that may have occurred on the continental shelf during the LGP, it simplifies all the information into a single spatial analysis and a single cartographic output, which can be improved with better input data if available.

The extreme variability of certain areas such as the Strait of Sicily or the Aegean Islands highlights the need for future analyses focused on straits, due to their evident importance in the interpretation of human migrations and all types of fauna during such a unique period of prehistory.

## FUNDING DECLARATION

This article was developed without additional funding, within the context of the project “Discovering the Deep Mediterranean Environment: A History of Science and Strategy (1860-2020) - DEEPMED (101002330)”.

## COMPETING INTEREST DECLARATION

The authors declare no competing interests.

## REFERENCES

- Acer Y., 2017. *The Aegean Maritime Disputes and International Law*. Routledge, New York, 304 pp.
- Antonioli F., Chiocci F.L., Anzidei M., Capotondi L., Casalbore D., Magri D., Silenzi S., 2017. *The central mediterranean*. In: Flemming N.C., Harff J., Moura D., Burgess A., Bailey G.N. (Eds), *Submerged Landscapes of the European Continental Shelf. Quaternary Paleoenvironments*, 341-376. Wiley-Blackwell, Chichester, 475 pp.
- Argus D.F., Peltier W.R., 2010. *Constraining models of postglacial rebound using space geodesy: a detailed assessment of model ICE-5G (VM2) and its relatives*. *Geophysical Journal International*, 181 (2), 697-723. <https://doi.org/10.1111/j.1365-246X.2010.04562.x>
- Badhani S., Cattaneo A., Dennielou B., Leroux E., Colin F., Thomas Y., Jouet G., Rabineau M., Droz L., 2020. *Morphology of retrogressive failures in the Eastern Rhone interfluvium during the LGM (Gulf of Lions, Western Mediterranean)*. *Geomorphology*, 351, 106894. <https://doi.org/10.1016/j.geomorph.2019.106894>
- Bardají T., Cabero A., Lario J., Zazo C., Silva P.G., Goy J.L., Dabrio C.J., 2015. *Coseismic vs. climatic factors in the record of relative sea level changes: An example from the Last Interglacials in SE Spain*. *Quaternary Science Reviews*, 113, 60-77. <https://doi.org/10.1016/j.quascirev.2014.10.005>
- Benjamin J., Rovere A., Fontana A., Furlani S., Vacchi M., Inglis R.H., Gehrels R., 2017. *Late Quaternary sea-level changes and early human societies in the central and eastern Mediterranean Basin: An interdisciplinary review*. *Quaternary International*, 449, 29-57. <https://doi.org/10.1016/j.quaint.2017.06.025>
- Bird M.I., Beaman R.J., Condie S.A., Cooper A., Ulm S., Veth P., 2018. *Palaeogeography and voyage modeling indicates early human colonization of Australia was likely from Timor-Roti*. *Quaternary Science Reviews*, 191, 431-439. <https://doi.org/10.1016/j.quascirev.2018.04.027>
- Björck S., Lambeck K., Möller P., Waldmann N., Bennike O., Jiang H., Porter C.T., 2021. *Relative sea level changes and glacio-isostatic modelling in the Beagle Channel, Tierra del Fuego, Chile: Glacial and tectonic implications*. *Quaternary Science Reviews*, 251, 106657. <https://doi.org/10.1016/j.quascirev.2020.106657>
- Çağatay M.N., Görür N., Algan O., Eastoe C., Tchapylyga A., Ongan D., Kuhn T., Kuşçu I., 2000. *Late Glacial-Holocene palaeoceanography of the Sea of Marmara: Timing of connections with the Mediterranean and the Black Seas*. *Marine Geology*, 167 (3-4), 191-206. [https://doi.org/10.1016/S0025-3227\(00\)00031-1](https://doi.org/10.1016/S0025-3227(00)00031-1)

- Camafort M., Ranero C.R., Gràcia E., 2022. *Active tectonics of the North Tunisian continental margin*. *Tectonics*, 41 (4), e2021TC007110. <https://doi.org/10.1029/2021TC007110>
- Clague J.J., Ward B., 2011. *Pleistocene glaciation of british Columbia*. In: *Developments in Quaternary Sciences*, 15, 563-573, Elsevier, Amsterdam, 1108 pp.
- Clark P.U., Mix A.C., 2002. *Ice sheets and sea level of the Last Glacial Maximum*. *Quaternary Science Reviews*, 21 (1-3), 1-7. [https://doi.org/10.1016/S0277-3791\(01\)00118-4](https://doi.org/10.1016/S0277-3791(01)00118-4)
- Clement A.C., Peterson L.C., 2008. *Mechanisms of abrupt climate change of the LGM*. *Reviews of Geophysics*, 46 (4). <https://doi.org/10.1029/2006RG000204>
- Colantoni P., Galignani P., Lenaz R., 1979. *Late Pleistocene and Holocene evolution of the North Adriatic continental shelf (Italy)*. *Marine Geology*, 33 (1-2), M41-M50. [https://doi.org/10.1016/0025-3227\(79\)90130-0](https://doi.org/10.1016/0025-3227(79)90130-0)
- Cooper J.A.G., Green A.N., Compton J.S., 2018. *Sea-level change in southern Africa since the LGM*. *Quaternary Science Reviews*, 201, 303-318. <https://doi.org/10.1016/j.quascirev.2018.10.013>
- Coronato A., Meglioli A., Rabassa J., 2004. *Glaciations in the Magellan Straits and Tierra del Fuego, southernmost South America*. *Developments in Quaternary Sciences*, 2, 45-48. [https://doi.org/10.1016/S1571-0866\(04\)80110-6](https://doi.org/10.1016/S1571-0866(04)80110-6)
- Deiana G., Lecca L., Melis R.T., Soldati M., Demurtas V., Orrù P.E., 2021. *Submarine geomorphology of the southwestern Sardinian continental shelf (Mediterranean Sea): Insights into the LGM sea-level changes and related environments*. *Water*, 13 (2), 155. <https://doi.org/10.3390/w13020155>
- Ding K., Freymueller J.T., He P., Wang Q., Xu C., 2019. *Glacial isostatic adjustment, intraplate strain, and relative sea level changes in the eastern United States*. *Journal of Geophysical Research: Solid Earth*, 124 (6), 6056-6071. <https://doi.org/10.1029/2018JB017060>
- Domzig A., Yelles K., Le Roy C., Déverchère J., Bouillin J.P., Bracène R., Pauc H., 2006. *Searching for the Africa-Eurasia Miocene boundary offshore western Algeria (MARADJA'03 cruise)*. *Comptes Rendus Geoscience*, 338 (1-2), 80-91. <https://doi.org/10.1016/j.crte.2005.11.009>
- Donnici S., Barbero R.S., 2002. *The benthic foraminiferal communities of the northern Adriatic continental shelf*. *Marine Micropaleontology*, 44 (3-4), 93-123. [https://doi.org/10.1016/S0377-8398\(01\)00043-3](https://doi.org/10.1016/S0377-8398(01)00043-3)
- Dutton A., Villa A., Chutcharavan P.M., 2022. *Compilation of Last Interglacial (Marine Isotope Stage 5e) sea-level indicators in the Bahamas, Turks and Caicos, and the east coast of Florida, USA*. *Earth System Science Data*, 14 (5), 2385-2399. <https://doi.org/10.5194/essd-14-2385-2022>
- Enrichetti F., Dominguez-Carrión C., Toma M., Bavestrello G., Canese S., Bo M., 2020. *Assessment and distribution of seafloor litter on the deep Ligurian continental shelf and shelf break (NW Mediterranean Sea)*. *Marine Pollution Bulletin*, 151, 110872. <https://doi.org/10.1016/j.marpolbul.2019.110872>
- Ercilla G., Díaz J.I., Alonso B., Farran M.L., 1995. *Late Pleistocene-Holocene sedimentary evolution of the northern Catalonia continental shelf (northwestern Mediterranean Sea)*. *Continental Shelf Research*, 15 (11-12), 1435-1451. [https://doi.org/10.1016/0278-4343\(94\)00089-6](https://doi.org/10.1016/0278-4343(94)00089-6)
- Ergin M., Kazan B., Ediger V., 1996. *Source and depositional controls on heavy metal distribution in marine sediments of the Gulf of Iskenderun, Eastern Mediterranean*. *Marine Geology*, 133 (3-4), 223-239. [https://doi.org/10.1016/0025-3227\(96\)00011-4](https://doi.org/10.1016/0025-3227(96)00011-4)
- Erlanson J.M., Braje T.J., 2015. *Coasting out of Africa: The potential of mangrove forests and marine habitats to facilitate human coastal expansion via the Southern Dispersal Route*. *Quaternary International*, 382, 31-41. <https://doi.org/10.1016/j.quaint.2015.03.046>
- Foutrakis P.M., Anastakis G., 2020. *Quaternary continental shelf basins of Saronikos Gulf, Aegean Sea*. *Geo-Marine Letters*, 40 (5), 629-647. <https://doi.org/10.1007/s00367-020-00653-9>
- Fraille-Jurado P., Mejías-García J.C., 2022. *Método para el cálculo, análisis y representación espacial de la variable " tiempo sumergido bajo el nivel del mar durante la última glaciación" en la plataforma continental del Golfo de Cádiz (España y Portugal)*. *Revista de Geografía Norte Grande*, 81, 183-205. <http://dx.doi.org/10.4067/S0718-34022022000100183>
- Fraille-Jurado P., Sánchez-Carnero N., Ojeda-Zújar J., 2014. *Sensibilidad del cálculo de los niveles medios del mar al método y período de las series temporales de los mareógrafos en los procesos de inundación: Valdelagrana (Cádiz)*. *Boletín de la Asociación de Geógrafos Españoles*, 65, 59-70. <https://doi.org/10.21138/bage.1743>
- Fraille-Jurado P., Ojeda-Zújar J., 2013. *The importance of the vertical accuracy of digital elevation models in gauging inundation by sea level rise along the Valdelagrana beach and marshes (Bay of Cádiz, SW Spain)*. *Geo-Marine Letters*, 33, 225-230. <https://doi.org/10.1007/s00367-012-0317-8>
- Frihy O.E., Nasr S.M., Ahmed M.H., El Raey M., 1991. *Temporal shoreline and bottom changes of the inner continental shelf off the Nile Delta, Egypt*. *Journal of Coastal Research*, 7 (2), 465-475. <https://www.jstor.org/stable/4297835>
- Garcea E.A., 2012. *Successes and failures of human dispersals from North Africa*. *Quaternary International*, 270, 119-128. <https://doi.org/10.1016/j.quaint.2011.06.034>
- Geopolis A.A., 1988. *Delimitation of the Continental Shelf in the Aegean Sea*. *Fordham International Law Journal*, 12 (1), 90-126. <https://ir.lawnet.fordham.edu/ilj/vol12/iss1/5>
- Gros L., 1977. *The dispute between Greece and Turkey concerning the continental shelf in the Aegean*. *American Journal of International Law*, 71 (1), 31-59. <https://doi.org/10.2307/2200324>
- Halouani N., Fathallah S., Gueddari M., 2012. *Beach and nearshore morphodynamic changes of the Tabarka coast, Northwest of Tunisia*. *Environmental Earth Sciences*, 66 (4), 1059-1069. <https://doi.org/10.1007/s12665-011-1312-5>
- Head M.J., 2021. *Review of the Early-Middle Pleistocene boundary and Marine Isotope Stage 19*. *Progress in Earth and Planetary Science*, 8 (1), 1-38. <https://doi.org/10.1186/s40645-021-00439-2>
- Hughes P.D., Gibbard P.L., Ehlers J., 2013. *Timing of glaciation during the last glacial cycle: Evaluating the concept of a global 'LGM' (LGM)*. *Earth Science Reviews*, 125, 171-198. <https://doi.org/10.1016/j.earsci-rev.2013.07.003>
- Ishiya T., Yokoyama Y., Okuno J.I., Obrochta S., Uehara K., Ikehara M., Miyairi Y., 2019. *A sea-level plateau preceding the Marine Isotope Stage 2 minima revealed by Australian sediments*. *Scientific Reports*, 9 (1), 6449. <https://doi.org/10.1038/s41598-019-42573-4>
- Khan N.S., Horton B.P., Engelhart S., Rovere A., Vacchi M., Ashe E.L., Tornqvist T.E., Dutton A., Hijma M.P., Shennan I., 2019. *Inception of a global atlas of sea levels since the LGM*. *Quaternary Science Reviews*, 220, 359-371. <https://doi.org/10.1016/j.quascirev.2019.07.016>
- Kholeif S.E.H., Ibrahim M.I., 2010. *Palyofacies analysis of inner continental shelf and middle slope sediments offshore Egypt, south-eastern Mediterranean*. *Geobios*, 43 (3), 333-347. <https://doi.org/10.1016/j.geobios.2009.10.006>
- Lafosse M., Gorini C., Le Roy P., Alonso B., d'Acremont E., Ercilla G., Ammar A., 2018. *Late Pleistocene-Holocene history of a tectonically active segment of the continental margin (Nekor basin, Western Mediterranean, Morocco)*. *Marine and Petroleum Geology*, 97, 370-389. <https://doi.org/10.1016/j.marpetgeo.2018.07.022>
- Lambeck K., Rouby H., Purcell A., Sun Y., Sambridge M., 2014. *Sea level and global ice volumes from the Last Glacial Maximum to the Ho-*

- locene. Proceedings of the National Academy of Sciences, 111 (43), 15296-15303. <https://doi.org/10.1073/pnas.1411762111>
- Leanza U., 1993. *The delimitation of the continental shelf of the Mediterranean Sea*. The International Journal of Marine and Coastal Law, 8 (3), 373-395.
- Li Z., Peng Z., Zhang Z., Chu Y., Xu C., Yao S., Ma J., 2023. *Exploring modern bathymetry: A comprehensive review of data acquisition devices, model accuracy, and interpolation techniques for enhanced underwater mapping*. Frontiers in Marine Science, 10, 1178845. <https://doi.org/10.3389/fmars.2023.1178845>
- Lipej L., Kovacic M., Dulcic J., 2022. *An analysis of adriatic ichthyofauna – Ecology, zoogeography, and conservation status*. Fishes, 7 (2), 58. <https://doi.org/10.3390/fishes7020058>
- Lobo F.J., Fernández-Salas L.M., Moreno I., Sanz J.L., Maldonado A., 2006. *The sea-floor morphology of a Mediterranean shelf fed by small rivers, northern Alboran Sea margin*. Continental Shelf Research, 26 (20), 2607-2628. <https://doi.org/10.1016/j.csr.2006.08.006>
- Lodolo E., Loreto M.F., Melini D., Spada G., Civile D., 2022. *Palaeo-Shoreline Configuration of the Adventure Plateau (Sicilian Channel) at the LGM*. Geosciences, 12 (3), 125. <https://doi.org/10.3390/geosciences12030125>
- Malanotte-Rizzoli P. 1991. *The Northern Adriatic Sea as a prototype of convection and water mass formation on the continental shelf*. Elsevier Oceanography Series, 57, 229-239.
- Mandryk C.A., Josenhans H., Fedje D.W., Mathewes R.W., 2001. *Late Quaternary paleoenvironments of Northwestern North America: Implications for inland versus coastal migration routes*. Quaternary Science Reviews, 20 (1-3), 301-314. [https://doi.org/10.1016/S0277-3791\(00\)00115-3](https://doi.org/10.1016/S0277-3791(00)00115-3)
- Mann T., Bender M., Lorscheid T., Stocchi P., Vacchi M., Switzer A.D., Rovere A., 2019. *Holocene sea levels in southeast Asia, Maldives, India and Sri Lanka: the SEAMIS database*. Quaternary Science Reviews, 219, 112-125. <https://doi.org/10.1016/j.quascirev.2019.07.007>
- Marchese F., Bracchi V.A., Lisi G., Basso D., Corselli C., Savini A., 2020. *Assessing fine-scale distribution and volume of Mediterranean algal reefs through terrain analysis of multibeam bathymetric data. A case study in the southern Adriatic continental shelf*. Water, 12 (1), 157. <https://doi.org/10.3390/w12010157>
- McCulloch R.D., Fogwill C.J., Sugden D.E., Bentley M.J., Kubik P.W., 2005. *Chronology of the last glaciation in central Strait of Magellan and Bahía Inútil, southernmost South America*. Geografiska Annaler: Series A, Physical Geography, 87 (2), 289-312. <https://doi.org/10.1111/j.0435-3676.2005.00260.x>
- McGinley G.P., 1985. *Intervention in the International Court: The Libya/Malta Continental Shelf Case*. International & Comparative Law Quarterly, 34 (4), 671-694.
- Mörner N.A., 2021. *Recorded sea level variability in the Holocene and expected future changes*. In: Eisma D. (Ed.), Climate Change Impact on Coastal Habitation, 17-28, CRC Press, London, 270 pp.
- Ostanciaux E., Husson L., Choblet G., Robin C., Pedoja K., 2012. *Present-day trends of vertical ground motion along the coast lines*. Earth-Science Reviews, 110 (1-4), 74-92. <https://doi.org/10.1016/j.earscirev.2011.10.004>
- Peltier W.R., 2002. *Global glacial isostatic adjustment: Palaeogeodetic and space-geodetic tests of the ICE-4G (VM2) model*. Journal of Quaternary Science, 17 (5-6), 491-510. <https://doi.org/10.1002/jqs.713>
- Pellegrini C., Tesi T., Schieber J., Bohacs K.M., Rovere M., Asioli A., ..., Trincardi F., 2021. *Fate of terrigenous organic carbon in muddy clinothems on continental shelves revealed by stratigraphic geometries: Insight from the Adriatic sedimentary archive*. Global and Planetary Change, 203, 103539. <https://doi.org/10.1016/j.gloplacha.2021.103539>
- Pérez-Mejías C., Moreno A., Sancho C., Martín-García R., Spötl C., Cacho I., Edwards R.L., 2019. *Orbital-to-millennial scale climate variability during Marine Isotope Stages 5 to 3 in northeast Iberia*. Quaternary Science Reviews, 224, 105946. <https://doi.org/10.1016/j.quascirev.2019.105946>
- Pico T., Mitrovica J.X., Mix A.C., 2020. *Sea level fingerprinting of the Bering Strait flooding history detects the source of the Younger Dryas climate event*. Science Advances, 6 (9), eaay2935. <https://www.science.org/doi/10.1126/sciadv.aay2935>
- Rabineau M., Berné S., Aslanian D., Olivet J.L., Joseph P., Guillocheau F., Granjeon D., 2005. *Sedimentary sequences in the Gulf of Lion: A record of 100,000 years climatic cycles*. Marine and Petroleum Geology, 22 (6-7), 775-804. <https://doi.org/10.1016/j.marpetgeo.2005.03.010>
- Riechers K., Mitsui T., Boers N., Ghil M., 2022. *Orbital insolation variations, intrinsic climate variability, and Quaternary glaciations*. Climate of the Past, 18 (4), 863-893. <https://doi.org/10.5194/cp-18-863-2022>
- Roach J.A., Smith R.W., 1994. *Chapter II: Identification of Excessive Maritime Claims*. In: Roach J.K., Smith R.W. (Eds), International Law Studies, Vol. 66, 11-19.
- Segev A., Rybakov M., Lyakhovskiy V., Hofstetter A., Tibor G., Goldshmidt V., Avraham Z.B., 2006. *The structure, isostasy and gravity field of the Levant continental margin and the southeast Mediterranean area*. Tectonophysics, 425 (1-4), 137-157. <https://doi.org/10.1016/j.tecto.2006.07.010>
- Setianto A., Triandini T., 2013. *Comparison of kriging and inverse distance weighted (IDW) interpolation methods in lineament extraction and analysis*. Journal of Applied Geology, 5 (1), 21-29. <https://doi.org/10.22146/jag.7204>
- Silva P.G., Bardají T., Roquero E., Baena-Preysler J., Cearreta A., Rodríguez-Pascua M.A., Rosas A., Zazo C. Goy J.L., 2017. *El periodo cuaternario: La historia geológica de la Prehistoria*. Cuaternario y Geomorfología, 31 (3.4), 113-154. <https://doi.org/10.17735/cyg.v31i3-4.55588>
- Simon K.M., James T.S., Dyke A.S., 2015. *A new glacial isostatic adjustment model of the Innuitian Ice Sheet, Arctic Canada*. Quaternary Science Reviews, 119, 11-21. <https://doi.org/10.1016/j.quascirev.2015.04.007>
- Sineo L., Petruso D., Forgia V., Messina A., D'Amore G., 2015. *Human peopling of Sicily during quaternary*. In: Quaternary Period, 25-67, Academy Publish Org.
- Talchabhadel R., Nakagawa H., Kawaike K., Yamanoi K., Thapa B.R., 2021. *Assessment of vertical accuracy of open source 30m resolution space-borne digital elevation models*. Geomatics, Natural Hazards and Risk, 12 (1), 939-960. <https://doi.org/10.1080/19475705.2021.1910575>
- Thiede J., 1978. *A glacial Mediterranean*. Nature, 276 (5689), 680-683.
- Ubilla M., Martínez S., 2016. *Geology and Paleontology of the Quaternary of Uruguay*. Springer International Publishing, Montevideo, 77 pp. <https://doi.org/10.1007/978-3-319-29303-5>
- Vergnaudgrazzini C., Caralp M., Faugeres J.C., Gonthier E., Grousset F., Pujol C., Saliège J.F., 1989. *Mediterranean outflow through the Strait of Gibraltar since 18000 years BP*. Oceanologica Acta, 12 (4), 305-324.
- Vilibić I., Zemunik P., Dunić N., Mihanović H., 2020. *Local and remote drivers of the observed thermohaline variability on the northern Adriatic shelf (Mediterranean Sea)*. Continental Shelf Research, 199, 104110. <https://doi.org/10.1016/j.csr.2020.104110>
- Yao Y., Harff J., Meyer M., Zhan W., 2009. *Reconstruction of paleocoastlines for the northwestern South China Sea since the LGM*. Science in China Series D: Earth Sciences, 52 (8), 1127-1136. <https://doi.org/10.1007/s11430-009-0098-8>

(Ms. received 28 June, accepted 24 September 2024)